Article:

Wagg, D.J. (2004) Rising phenomena and the multi-sliding bifurcation in a two-degree of freedom impact oscillator. Chaos, Solitons and Fractals, 22. 541 - 548. ISSN 0960-0779

https://doi.org/10.1016/j.chaos.2004.03.003

Chaos, Solitons and Fractals 22 (2004) 541–548

Rising phenomena and the multi-sliding bifurcation in a two-degree of freedom impact oscillator

D. J. Wagg*

Department of Mechanical Engineering, University of Bristol, Queens Building, University Walk, Bristol BS8 1TR, U.K.

May 3, 2013

Abstract

We consider the *rising* phenomena which occur in sticking solutions of a two-degree of freedom impact oscillator. We describe a mathematical formulation for modelling such a systems during both free flight and during sticking solutions for each of the masses in the system. Simulations of the sticking solutions are carried out, and rising events are observed when the forcing frequency parameter is varied. We show how the time of sticking reduces significantly as a rising event occurs. Then within the sticking region we show how rising is qualitatively similar to the multi-sliding bifurcation for sliding orbits.

*Author for correspondance:David.Wagg@bristol.ac.uk

Chaos, Solitons and Fractals 22 (2004) 541–548

1 Introduction

In this paper we consider the so called *rising* phenomena which occur in sticking solutions of a two-degree of freedom impact oscillator. The impact oscillator consists of two masses, coupled with springs and dashpots, where the motion of both the masses is restricted by rigid constraints. Such systems have a range of applications as, for example, in machines with clearance and backlash [1]. Several authors have considered the nonlinear dynamics associated with two degree of freedom impact oscillators [2–5]. In particular, the bifurcation behaviour of two degree of freedom impact system with a single impact constraint has been studied in detail [6–8]. More general studies of multiple degree of freedom impact oscillators have also been carried out [9–11].

Chatter and sticking are phenomena which occur in a wide range of impact oscillator systems. Studies of chatter and sticking have been carried out for both single degree of freedom impact oscillators in [12] and for two degree of freedom systems by [13]. The behaviour of periodic sticking motions in both single and multi degree of freedom systems is considered by Toulemonde and Gontier [14], and the authors make reference to the "rising bifurcation" which they demonstrate occurs for a two degree of freedom system. It is this so called rising behaviour which forms the focus for the current study.

Sticking in impact systems is mathematically analogous to *sliding* in electrical systems [15]. The sliding orbits in these electrical systems have been shown to exhibit particular types of *sliding bifurcations* under parameter variation [16]. In fact there are four types of sliding bifurcation which can occur [17], for which the normal form mappings have been derived [18]. A *multi-sliding* bifurcation is one of the four cases, which occurs in the systems studied by [16–18], Previous physical manifestations of the multi-sliding bifurcation have been studied in models of relay feedback systems [16] and friction oscillators [19]. The multi-sliding bifurcation can also be related to the rising phenomena observed in vibro-impact systems — a connection which was first reported by [20]. In this paper, we examine the rising phenomena found in a two-degree of freedom vibro-impact system as a system parameter is varied, and find similar results to [14] regarding the drop in sticking time. We demonstrate using numerical simulations that rising and multi-sliding are qualitatively equivalent bifurcations events by observing that the sticking solutions become tangent to the boundary of the sticking region at a rising event — analogous to results for sliding orbits shown by [18].

2 Mathematical model

We consider a coupled two degree of freedom system, which is shown schematically in figure 1. The governing equations for the system away from impact can be expressed as

$$\ddot{x}_1 + \frac{c}{m}(2\dot{x}_1 - \dot{x}_2) + \frac{k}{m}(2x_1 - x_2) = \frac{A_1}{m}\cos(\Omega t), \tag{1}$$

$$\ddot{x}_2 + \frac{c}{m}(\dot{x}_2 - \dot{x}_1) + \frac{k}{m}(x_2 - x_1) = \frac{A_2}{m}\cos(\Omega t), \tag{2}$$

where x_1 represents the displacement of mass m_1 and x_2 the displacement of mass m_2 and we assume that $m_1 = m_2 = m$. The spring stiffnesses are given by $k_1 = k_2 = k$ and the damping by $c_1 = c_2 = c$ and the distance to the motion constraints are given by s_1 and s_2 respectively. Equation 2 has a dual condition for free flight that $(x_i - s_i) < 0$ for $s_i > 0$ and $(x_i - s_i) > 0$ for $s_i < 0$ which we will write as $(x_i - s_i) \lesseqgtr 0 \quad \forall s_i \gtreqless 0$.

Then equations (1) and (2) can be written in the form

$$[I]\ddot{\mathbf{x}} + \frac{c}{m}[E]\dot{\mathbf{x}} + \frac{k}{m}[E]\mathbf{x} = \frac{1}{m}\mathbf{f}(t), \quad (x_i - s_i) \lesseqgtr 0 \quad \forall s_i \gtreqless 0 \tag{3}$$

where $[E]$ is a 2×2 coupling matrix, $[I]$ is the identity matrix and $\mathbf{f}(t) = \mathbf{A}\cos(\Omega t)$, where $\mathbf{A} = \{A_1, A_2\}^T$. Note: $A_2 = 0$ for all the simulations in this paper.

The natural frequencies are given by $\omega_{nj} = \sqrt{\lambda_j k/m}$ for $j = 1, 2$ where λ_j are the eigenvalues of matrix $[E]$, and the corresponding normalized eigenvectors ξ_j can be used to construct a orthogonal modal matrix $[\Psi] = [\{\xi_1\}, \{\xi_2\}]$. We can then transform equation

(3) into a modal form by defining modal coordinates $\mathbf{q} = \{q_1, q_2\}^T$, such that $\mathbf{x} = [\Psi]\mathbf{q}$ and

$$[I]\ddot{\mathbf{q}} + \frac{c}{m}[\Lambda]\dot{\mathbf{q}} + \frac{k}{m}[\Lambda]\mathbf{q} = \frac{1}{m}[\Psi]^T\mathbf{f}(t) \qquad (4)$$

where $[\Lambda] = [\Psi]^T[E][\Psi]$ is the diagonal matrix of the eigenvalues, λ_j, $j = 1, 2$.

In this modal formulation, we define the vector $\psi_i = \{\Psi_{i1}, \Psi_{i2}\}^T$, such that an impact occurs when $\psi_i^T\mathbf{q} = x_i$, $i = 1, 2$. Hence equation (4) is valid only for $(\psi_i^T\mathbf{q} - s_i) \lesseqgtr 0 \quad \forall s_i \gtreqless 0$, which is equivalent to the condition that $(x_i - s_i) \lesseqgtr 0 \quad \forall s_i \gtreqless 0$ for the ith impacting mass.

We can simplify equation (4) such that for each mode

$$\ddot{q}_j + 2\zeta_j\omega_{nj}\dot{q}_j + \omega_{nj}^2 q_j = \frac{\hat{f}_j}{m}\cos(\Omega t), \quad j = 1, 2, \qquad (5)$$

where $\hat{\mathbf{f}} = [\Psi]^T\mathbf{A}$, $\hat{\mathbf{f}} = \{\hat{f}_1, \hat{f}_2\}^T$ and $\zeta_j = (c/2)\sqrt{\lambda_j/km}$ is the modal damping coefficient. Equation (5) has the well known exact solution for under-damped oscillations $0 < \zeta_j < 1$ [21], so that we can solve for each mode exactly, and hence find the total displacements x_1, x_2 — see [13, 22] for further details. Without loss of generality, this formulation can be considered in either a dimensional or a nondimensional form [22] — in the following work we assume all parameters and variables are nondimensional.

2.1 Modelling impact events

When $(x_i - s_i) = 0$ for $i = 1, 2$ an impact occurs and an instantaneous coefficient of restitution rule is applied. A single isolated impact occurs when for the ith mass $x_i = s_i$, while for $j \neq i$:$(x_j - s_j) \lesseqgtr 0 \quad \forall s_j \gtreqless 0$. This type of impact may be modelled using an instantaneous coefficient of restitution rule [23] such that

$$\dot{x}_i(t_+) = -r\dot{x}_i(t_-) \quad x_i = s_i \qquad (6)$$

where, t_- is the time just before impact, t_+ is the time just after impact and r is the coefficient of restitution with a value in the range $r \in [0, 1]$. In matrix form the coefficient of restitution rule can be written as

$$\dot{\mathbf{x}}(t_+) = [R_k]\dot{\mathbf{x}}(t_-) \tag{7}$$

where for the systems being considered there are three different cases for the $[R_k]$ matrices

$$[R_1] = \begin{bmatrix} -r & 0 \\ 0 & 1 \end{bmatrix}, \quad [R_2] = \begin{bmatrix} 1 & 0 \\ 0 & -r \end{bmatrix}, \quad [R_3] = \begin{bmatrix} -r & 0 \\ 0 & -r \end{bmatrix}. \tag{8}$$

corresponding to mass 1 impacting, mass 2 impacting and simultaneous impact of both masses.

In modal form the coefficient of restitution rule, equation 7, becomes

$$[\Psi]\dot{\mathbf{q}}(\tau_+) = [R_k][\Psi]\dot{\mathbf{q}}(\tau_-). \tag{9}$$

This leads to the relation for the modal velocities after impact

$$\dot{\mathbf{q}}(\tau_+) = [\hat{R}_k]\dot{\mathbf{q}}(\tau_-), \tag{10}$$

where $[\hat{R}_k] = [\Psi]^{-1}[R_k][\Psi]$ is the set of matrices which represents a linear transform of modal velocities just before impact to modal velocities just after impact for the 3 possible impact cases.

2.2 Sticking solutions

For this system there are two possible sticking regimes; when $x_1 = s_1$ and when $x_2 = s_2$. There is also a dual sticking regime when both $x_1 = s_1$ and $x_2 = s_2$ simultaneously, but this will not be considered here. Each regime has a reduced set of governing equations with explicit solutions [22].

In the case where mass 1 sticks $x_1 = s_1$ and $\dot{x}_1 = 0$, so that the equations of motion reduce to a single equation; equation (2) which becomes (with $A_2 = 0$)

$$\ddot{x}_2 + \frac{c}{m}\dot{x}_2 + \frac{k}{m}(x_2 - s_1) = 0. \tag{11}$$

The force which holds the mass against the stop during sticking, from equation (1) is given by

$$F_2 = c\dot{x}_2 + k(x_2 - 2s_1) + A_1\cos(\Omega t). \tag{12}$$

Equation (11) has the exact solution

$$x_2 = e^{-\hat{\zeta}\hat{\omega}_n(t-t_s)}(C_1\cos(\hat{\omega}_d(t-t_s)) + C_2\sin(\hat{\omega}_d(t-t_s))) + s_1, \tag{13}$$

where $\hat{\omega}_n = \sqrt{k/m}$, $\hat{\zeta} = c/2m\hat{\omega}_n$ and $\hat{\omega}_d = \hat{\omega}_n\sqrt{1-\hat{\zeta}^2}$. At the start of the sticking period $t_s = t$ and the constants C_1 and C_2 can be found using the initial conditions $x_1(t_s) = s_1$ and $\dot{x}_1(t_s) = 0$.

The change from free motion of both masses to one mass sticking represents a reduction in the degree of freedom of the system from 2 to 1. The initial conditions for equation (13) can be taken directly from the values of x_2 and $\dot{x}_2$ immediately prior to a sticking phase when $x_1 = s_1$ and $\dot{x}_1 = 0$. The sticking phase ends when F_2 becomes zero and changes sign at which time $t = t_f$.

In the case $x_2 = s_2$ and $\dot{x}_2 = 0$, the reduced equation of motion is given by

$$\ddot{x}_1 + 2\frac{c}{m}\dot{x}_1 + \frac{k}{m}(2x_1 - s_2) = \frac{A_1}{m}\cos(\Omega t). \tag{14}$$

The force which holds the mass against the stop during sticking is given by

$$F_1 = c\dot{x}_1 + k(x_1 - s_2). \tag{15}$$

Equation (14) has the exact solution

$$x_1 = e^{-2\hat{\zeta}\hat{\omega}_n(t-t_s)}(C_1\cos(2\omega_d^*(t-t_s)) + C_2\sin(2\omega_d^*(t-t_s))) + C_3\cos(\Omega t - \phi^*) - s_2/2, \tag{16}$$

where $\hat{\omega}_n = \sqrt{k/m}$, $\hat{\zeta} = c/2m\hat{\omega}_n$, $\omega_d^* = \hat{\omega}_n\sqrt{0.5-\hat{\zeta}^2}$, t_0 is taken at the start of the sticking period and

$$\phi^* = \arctan\left(\frac{4\hat{\zeta}(\Omega/\hat{\omega}_n)}{2 - \Omega^2/\hat{\omega}_n^2}\right). \tag{17}$$

As with the preceding case the initial conditions for equation (13) can be taken directly from the values of x_1 and $\dot{x}_1$ immediately prior to a sticking phase when $x_2 = s_2$ and $\dot{x}_2 = 0$. These initial conditions allow us to compute the constants C_1, C_2 and C_3 [22].

3 The rising event

In this section we consider the example of a periodic sticking motion which exists for the parameter values $m_1 = m_2 = 1$, $k_1 = k_2 = 1$, $c_1 = c_2 = 0.1$, $s_1 = -0.3$, $s_2 = 0.1$, $r = 0.7$, forcing $A_1 = 0.5$ and $A_2 = 0.0$. At a forcing frequency of $\Omega = 0.255$ a periodic sticking motion exists. A time series of this periodic solution is shown in figure 2, and a phase portrait in figure 3. This periodic solution includes regions of free flight, chatter and sticking for both of the masses, although it should be noted that the sticking phases do not overlap (i.e. there is no dual sticking).

This particular sticking solution has been chosen as it is close to a rising event. The progression of the rising event as Ω is increased can be seen in figure 4. First we observe that as Ω is increased from 0.255 to 0.2561 the mass lifts off, or *rises*, part way through the sticking phase of the motion. After rising the mass goes into a chatter sequence and then sticks to the stop again. This means that the sticking phase of the periodic orbit is now composed of two separate parts. As Ω is increased further ($\Omega = 0.26$), the amplitude of the rise grows and the second part of the sticking phase reduces until only a single impact remains. Further increasing Ω beyond this point results in the loss of the single remaining impact such that only a single sticking phase is left.

This new sticking phase is significantly shorter than the original one, and [14] postulated that this sudden drop in sticking time is one way of identifying that a rising event had occurred. The sticking time for the frequency range considered in this example is shown in figure 5 (a) and (b), and a clear drop in sticking time can be seen at $\Omega \approx 0.26$ shown in close up in figure 5 (b). This is in agreement with results shown in [14]. From figure 5 (b), we can clearly see the two separate parts of the sticking orbit that occur after rising. i.e. there are two proportions of sticking time. One of the sticking time proportions can be see to decrease (approximately linearly) as the forcing frequency, Ω, is increased. At $\Omega \approx 0.2575$ this part of the sticking orbit reduces to zero, as we observe from the sequence of events shown in Figure 4.

4 The rising/multi-sliding bifurcation

The relationship $F_i = 0$ (equations 12 and 15) defines the boundary in phase space where sticking ends, which we denote as ∂S. For sticking to exist the condition $F_i s_i > 0$ must apply, which in this case is the region on the positive side of the boundary ∂S [22].

Considering sticking solutions in isolation from the rest of the periodic orbit, means that when a rising event occurs it can be considered as a bifurcation of the sticking solution. In figure 6 we have plotted the sticking solution for the rising example in figure 4 projected into $t, x_2, \dot{x}_2$: time, displacement and velocity. Here the solid line indicates the sticking orbit and the dashed line the boundary of the sticking region defined by ∂S. In figure 6 (a) the solution is just before rising, and in (b) just after rising. In each case the sticking solution coalesces with the boundary (i.e. it exits the sticking region) and in Figure 6 (a) the orbit comes very close to an additional tangential intersection with the boundary (i.e. just be for rising). In figure 6 (b) the orbit exits the region for a short time between $-0.2 \leq x_2 \leq -0.15$ — this is the post rising behaviour. We note also from Figure 6 that at the point of rising bifurcation the sticking orbit touches the boundary ∂S tangentially, as opposed to when it exits the region when the intersection with the boundary is transversal. The tangential nature of the rising event has similarities to the grazing bifurcation [24] which also occurs in these systems.

In fact this bifurcation is analogous to the *multi-sliding* bifurcation for sliding orbits, discussed by [16–18]. In the electrical systems exactly the same scenario occurs, where an orbit restricted to a switching manifold touches the boundary of the region tangentially at the point of bifurcation. Hence for sticking solutions we can refer to the occurrence of a rising bifurcation as a multi-sliding bifurcation.

5 Conclusions

In this paper we have considered rising phenomena which occur in sticking solutions of a two-degree of freedom impact oscillator. For this type of oscillator, exact solutions exist during the sticking phases of motion. We have shown numerical simulations of typical sticking solutions, and a rising event which occurs as the forcing frequency parameter is varied. From these numerical simulations we have observed similar results to [14] regarding the significant reduction in sticking time as a rising bifurcation occurs. In fact we have shown how the sticking time first separates into two distinct parts, one of which rapidly reduces to zero as the system parameter is increased. Within the sticking region we have shown how rising is qualitatively similar to the multi-sliding bifurcation for sliding orbits. This has been achieved by observing that the sticking solutions become tangent to the boundary of the sticking region at a rising event — analogous to previously published results for sliding orbits in relay feedback and friction oscillator systems.

6 Acknowledgements

This work was supported as part of an Advanced Research Fellowship from the EPSRC.

References

[1] S. Theodossiades and S. Natsiavas. Periodic and chaotic dynamics of motor-driven gear-pair system with backlash. *Chaos, Solitons and Fractals*, 12:2427–2440, 2001.

[2] J. Shaw and S. W. Shaw. The onset of chaos in a two-degree of freedom impacting system. *Journal of Applied Mechanics*, 56:168–174, 1989.

[3] S. F. Masri. Theory of the dynamic vibration neutraliser with motion-limiting stops. *Transactions of the American Society of Mechanical Engineers, Journal of Applied Mechanics*, 39:563–568, 1972.

[4] S. Chatterjee, A. K. Mallik, and A. Ghosh. On impact dampers for non-linear vibrating systems. *Journal of Sound and Vibration*, 187(3):403–420, 1995.

[5] R. D. Neilson and D. H. Gonsalves. Chaotic motion of a rotor system with a bearing clearance. In A. J. Crilly, R. A. Earnshaw, and H. Jones, editors, *Applications of fractals and chaos*, pages 285–303. Springer-Verlag, 1993.

[6] G. W. Luo and J. H. Xie. Hopf bifurcation of a two-degree-of-freedom vibro-impact system. *Journal of Sound and Vibration*, 213:391–408, 1998.

[7] G-L Wen. Codimension-2 hopf bifurcation of a two-degree-of-freedom vibro-impact system. *Journal of Sound and Vibration*, 242(3):475–485, 2001.

[8] G. W. Luo and J. H. Xie. Hopf bifurcations and chaos of a two-degree-of-freedom vibro-impact system in two strong resonance cases. *Non-linear Mechanics*, 37:19–34, 2002.

[9] J. P. Cusumano and B-Y. Bai. Period-infinity periodic motions, chaos and spatial coherence in a 10 degree of freedom impact oscillator. *Chaos, Solitons and Fractals*, 3:515–536, 1993.

[10] S. Natsiavas. Dynamics of multiple-degree-of-freedom oscillators with colliding components. *Journal of Sound and Vibration*, 165(3):439–453, 1993.

[11] D. Pun, S. L. Lua, S. S. Law, and D. Q. Cao. Forced vibration of a multidegree impact oscillator. *Journal of Sound and Vibration*, 213(3):447–466, 1998.

[12] C. J. Budd and F. Dux. Chattering and related behaviour in impact oscillators. *Philosophical Transactions of the Royal Society of London A*, 347:365–389, 1994.

[13] D. J. Wagg and S. R. Bishop. Chatter, sticking and chaotic impacting motion in a two-degree of freedom impact oscillator. *International Journal of Bifurcation and Chaos*, 11(1):57–71, 2001.

[14] C. Toulemonde and C Gontier. Sticking motions of impact oscillators. *European Journal of Mechanics A:Solids*, 17(2):339–366, 1998.

[15] M. Di Benardo, A. R. Champneys, and C. J. Budd. Grazing, skipping and sliding: analysis of the non-smooth dynamics of the dc/dc buck converter. *Nonlinearity*, 11(4):858–890, 1998.

[16] M. Di Bernardo, K. H. Johansson, and F. Vasca. Self-oscillations and sliding in relay feedback systems:symmetry and bifurcations. *International Journal of Bifurcation and Chaos*, 4(11):1121–1140, 2001.

[17] P. Kowalczyk and M. di Bernardo. On a novel class of bifurcations in hybrid dynamical systems. In *Lecture Notes in Computer Science*, number 2034, pages 361–374, 2001.

[18] M. Di Bernardo, P. Kowalczyk, and A. Nordmark. Bifurcations of dynamical systems with sliding: derivation of normal-form mappings. *Physica D*, 170:175–205, 2002.

[19] M. Di Bernardo, P. Kowalczyk, and A. Nordmark. Sliding bifurcations: A novel mechanism for the onset of chaos in dry friction oscillators. *International Journal of Bifurcation and Chaos*, 13(10):2935–2948, 2003.

[20] D. J. Wagg. Bifurcation phenomena in vibro-impact systems with multiple constraints. IMA conference on "Bifurcations: The use and control of chaos", Southampton, July 2003. To appear in proceedings., 2003.

[21] S. P. Timoshenko. *Vibration problems in engineering*. Van Nostrand, 1937.

[22] D. J. Wagg and S. R. Bishop. Dynamics of a two degree of freedom vibro-impact system with multiple motion limiting constraints. To appear in the International Journal of Bifurcation and Chaos, 2004.

[23] J. M. T. Thompson and H. B. Stewart. *Nonlinear dynamics and chaos*. Chichester: John Wiley, 2002.

[24] A. B. Nordmark. Non-periodic motion caused by grazing incidence in an impact oscillator. *Journal Of Sound and Vibration*, 145(2):275–297, 1991.

Figure Captions

- Figure 1 Schematic representation of an N degree of freedom impact oscillator with multiple motion limiting constraints.

- Figure 2 Example time series of sticking orbit for two degree of freedom system. Solid line x_2, broken line x_1. Parameters values $m_1 = m_2 = 1$, $k_1 = k_2 = 1$, $c_1 = c_2 = 0.1$, $x_s = 0.1$, $r = 0.7$, forcing $A_2 = 0.0$, $A_1 = 0.5$ and $\Omega = 0.255$.

- Figure 3 Phase portrait of time series shown in Figure 2. Solid line x_2, broken line x_1.

- Figure 5 Proportion of sticking time of mass 2 as a ratio of forcing period.

- Figure 4 Rising bifurcation in a two degree of freedom impact oscillator. Solid line x_2, broken line x_1. Parameter values $m_1 = m_2 = 1$, $k_1 = k_2 = 1$, $c_1 = c_2 = 0.1$, $x_s = 0.1$, $r = 0.7$, forcing $A_2 = 0.0$, $A_1 = 0.5$. (a) and (b) $\Omega = 0.255$; (c) and (d) $\Omega = 0.2561$; (e) and (f) $\Omega = 0.26$; (g) and (h) $\Omega = 0.27$.

- Figure 6 The sticking trajectories in $t, x_2\dot{x}_2$ space. Solid line sticking, dashed line $F_p = 0$ where $F_p = f(\dot{x}_2, x_2, t)$; (a) Just before rising for the case shown in figure 4 (a) and (b) and; (b) Just after rising for the case shown in figure 4 (c) and (d).

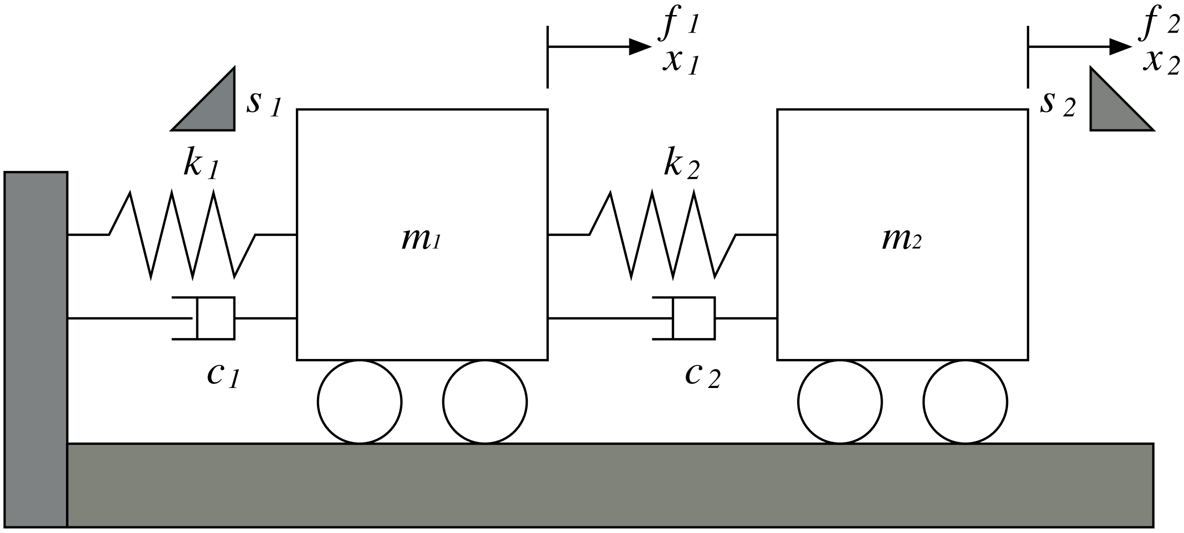

Figure 1:

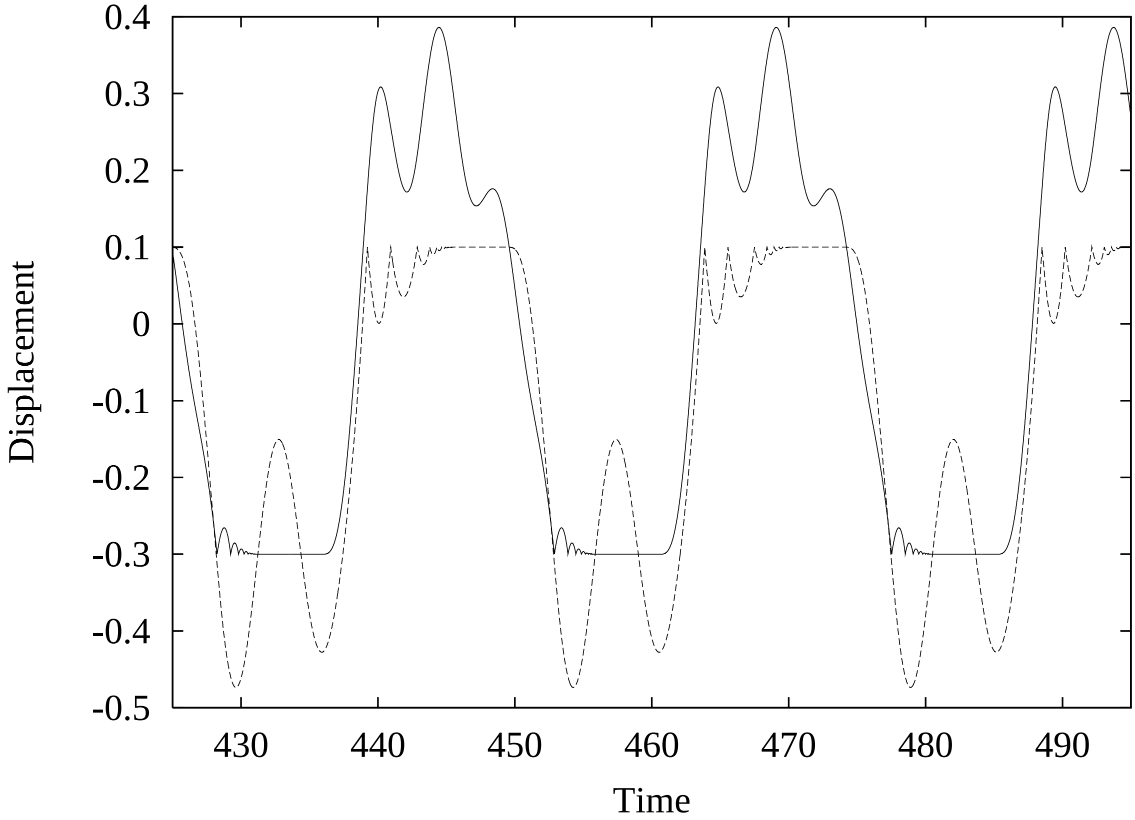
0.4
0.3
0.2
0.1
0
-0.1
-0.2
-0.3
-0.4
-0.5
Displacement
430
440
450
460
470
480
490
Time

Figure 2:

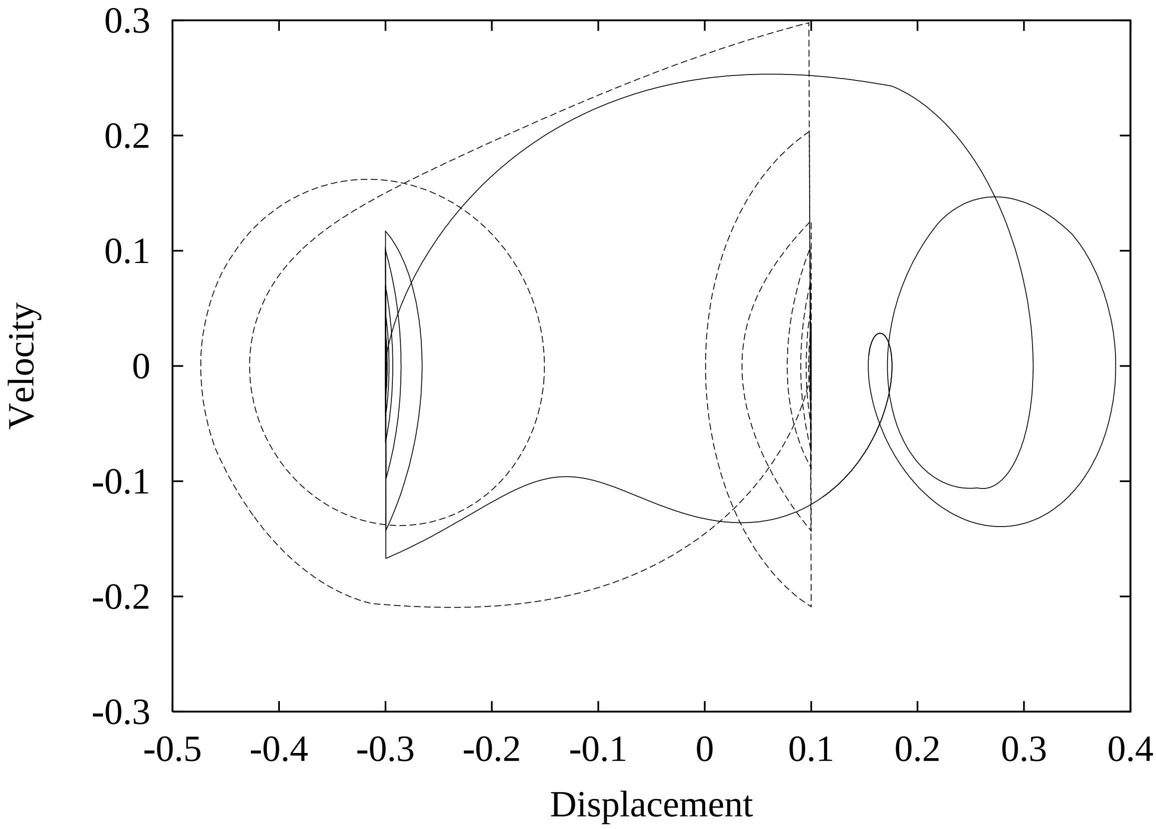
0.3
0.2
0.1
0
-0.1
-0.2
-0.3
Velocity
-0.5
-0.4
-0.3
-0.2
-0.1
0
0.1
0.2
0.3
0.4
Displacement

Figure 3:

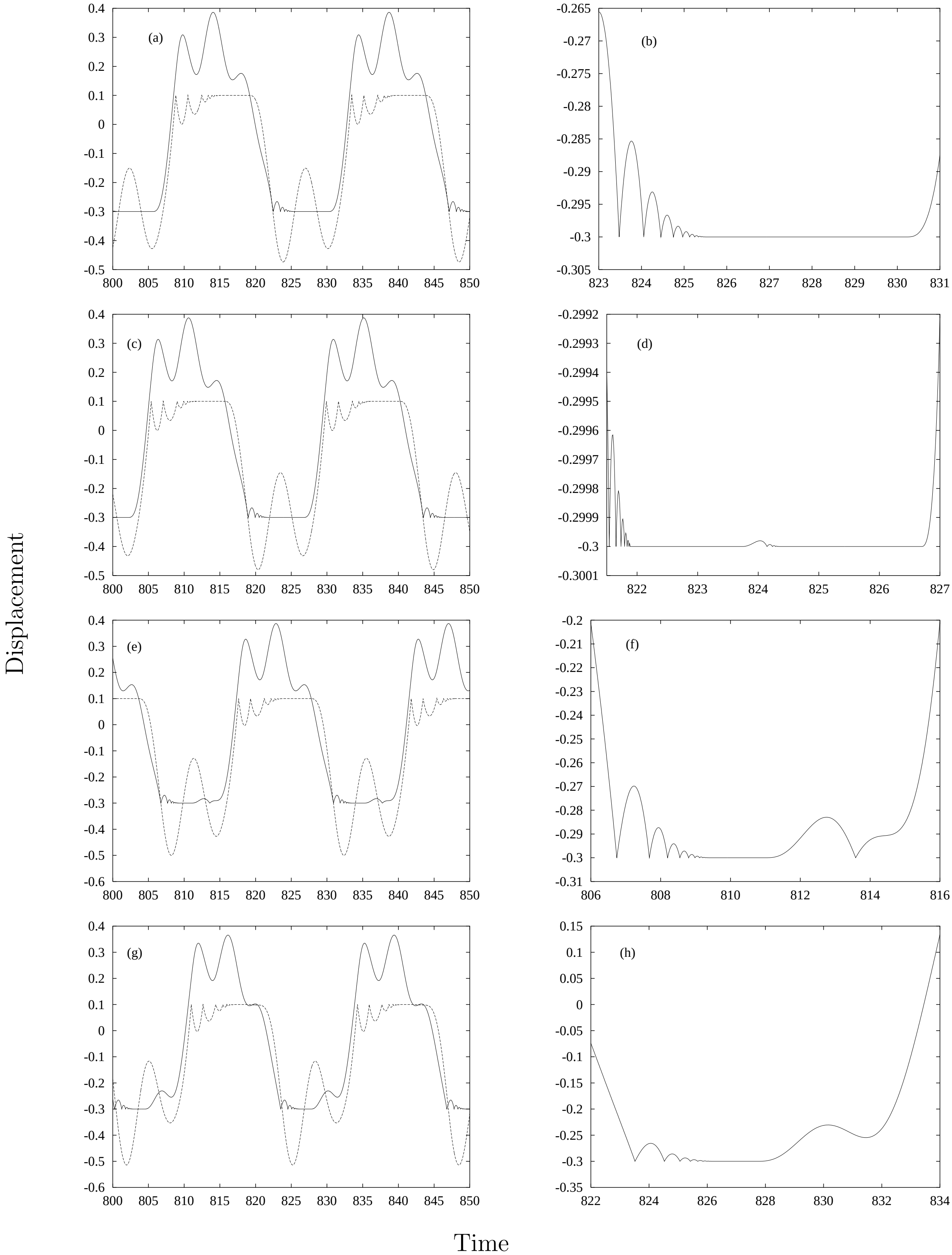

Figure 4:

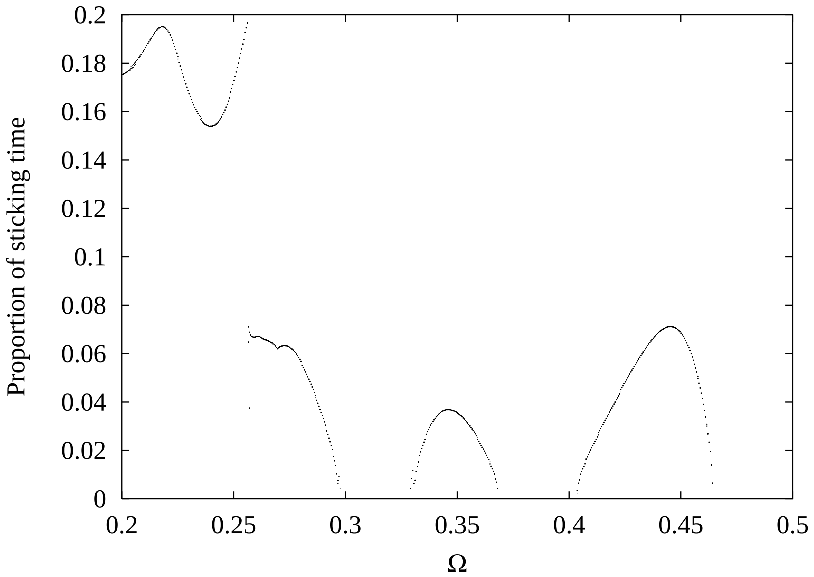

Proportion of sticking time
0.2
0.18
0.16
0.14
0.12
0.1
0.08
0.06
0.04
0.02
0
0.2
0.25
0.3
0.35
0.4
0.45
0.5
Ω

(a)

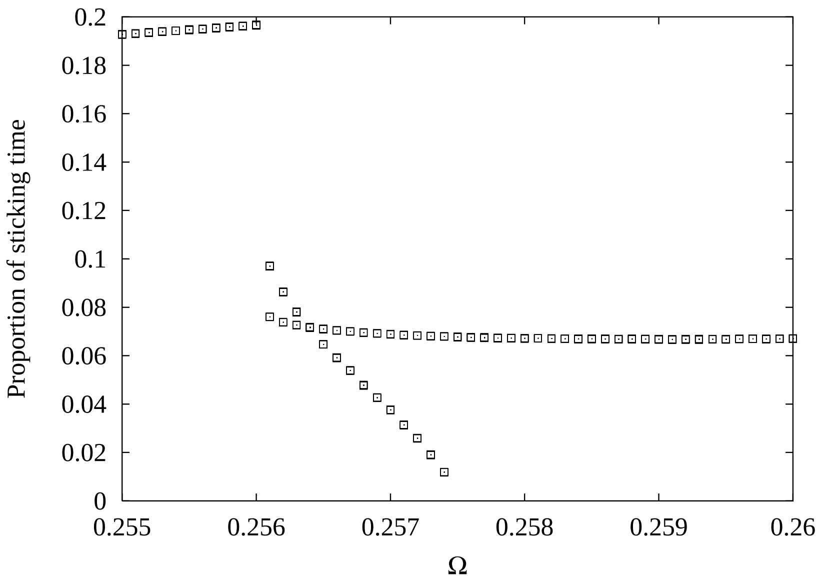

Proportion of sticking time
0.2
0.18
0.16
0.14
0.12
0.1
0.08
0.06
0.04
0.02
0
0.255
0.256
0.257
0.258
0.259
0.26
Ω

(b)

Figure 5:

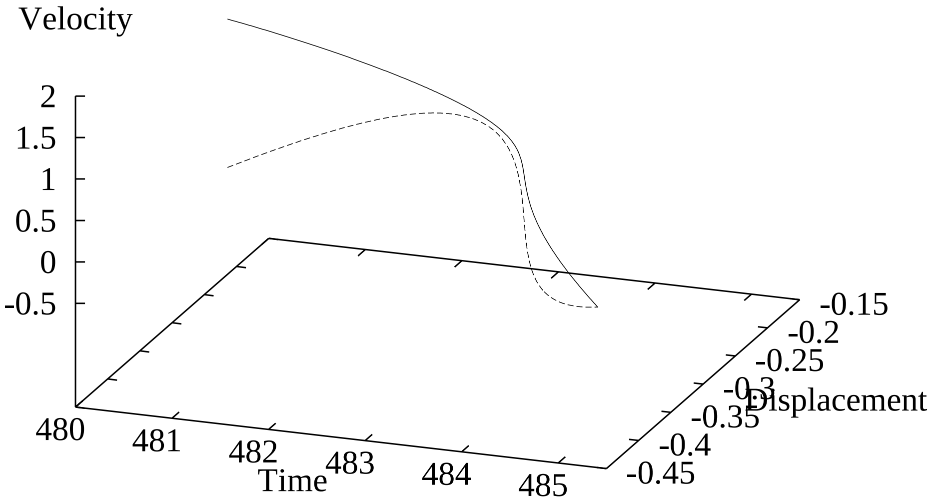
Velocity
2
1.5
1
0.5
0
-0.5
480
481
482
483
484
485
Time
-0.15
-0.2
-0.25
-0.3
-0.35
-0.4
-0.45
Displacement

(a)

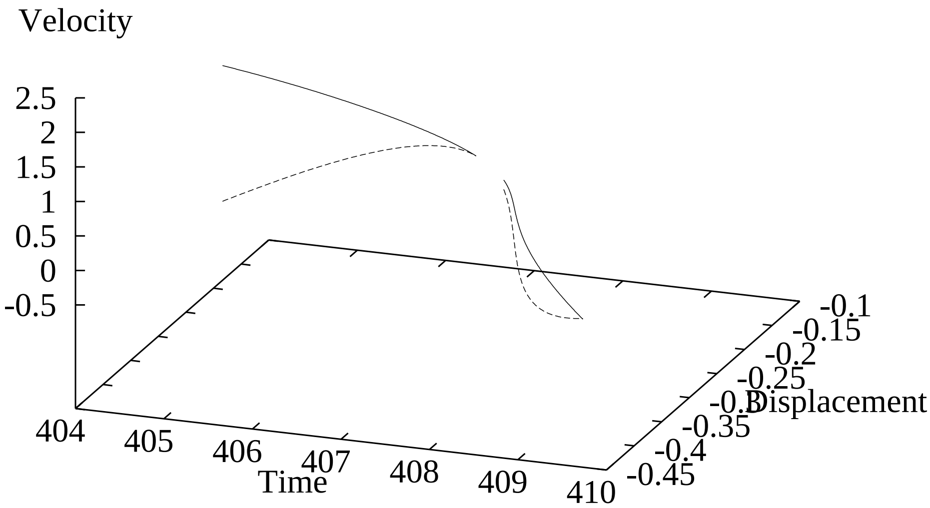
Velocity
2.5
2
1.5
1
0.5
0
-0.5
404
405
406
407
408
409
410
Time
-0.1
-0.15
-0.2
-0.25
-0.3
-0.35
-0.4
-0.45
Displacement

(b)

Figure 6: